Gaseous Photocatalytic Oxidation of Formic Acid over TiO_2: A Comparison between the Charge Carrier Transfer and Light-Assisted Mars–van Krevelen Pathways

Baoshun Liu,*[,†] Hao Wu,[†] and Ivan P. Parkin[‡]

[†]State Key Laboratory of Silicate Materials for Architectures, Wuhan University of Technology, Wuhan, Hubei 430070, P. R. China
[‡]Department of Chemistry, Materials Chemistry Centre, University College London, 20 Gordon St., London WC1H 0AJ, U.K.

Supporting Information

ABSTRACT: Under light illumination, it is usually considered that photocatalytic oxidations of organics such as volatile organic compounds over semiconductors are driven by the transfer of photogenerated carriers. Some studies also proposed that the photocatalytic oxidations might take place according to the light-assisted Mars–van Krevelen (MvK) pathway that involved the participation of lattice oxygens under aerobic conditions. Based on the concept of the MvK mechanism, the current work first gives an elaboration on the light-assisted MvK pathway and its intrinsic difference from the charge carrier transfer pathway. We then examined which one of these two mechanisms is responsible for the the photocatalytic oxidation of formic acid over TiO_2. Comprehensive experiments, including apparent kinetics, online electric conductances, vacuum electric conductances, online optical transmittances, and first principle calculations, were carried out to discuss this problem. The results showed that the photocatalytic oxidations of formic acid over TiO_2 dominantly follow the charge carrier transfer pathway at both low and elevated temperatures, the light-assisted MvK mechanism could not play a major role, and there was also no transition from the charge carrier transfer to the light-assisted MvK mechanism with an increase of reaction temperature.

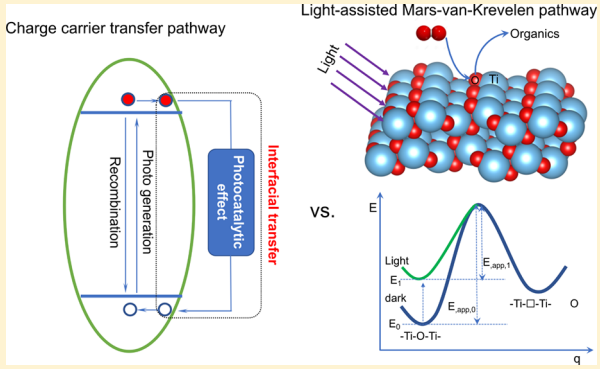

1. INTRODUCTION

Upon UV light illumination, many oxide materials can be used to oxidize organics such as volatile organic compounds (VOCs) due to the function of the photocatalytic effect.[1−5] It has been usually accepted that the photocatalytic oxidations of VOCs happen via the pathway of charge carrier transfer.[6−9] The mechanism of the charge carrier transfer pathway is shown in Figure 1A. In this pathway, the photocatalytic effect is a result of electron transfer from the conduction band (CB) to the valence band (VB) of semiconductors.[10,11] The electron transfer leads to a generation of various oxidative radicals (or species) that include superoxide O_2^-, O^- (electron trapped at dissociated oxygen atom or lattice oxygens), hydroxyl radicals (·OH), O_3^{3-}, and others,[6−9] which can then react with organics. The intrinsic feature of this mechanism is that the photoinduced charge carriers, the holes and electrons, must go out of the photocatalysts together to participate in photocatalysis, independent on the specific pathways of charge carrier transfer.

Some studies suggested that the photocatalytic oxidations of benzene over TiO_2, happening via the charge carrier transfer pathway, might decrease as the temperature increased.[12,13] They saw that the photocatalytic oxidations at elevated temperatures were more efficient than those at ambient (or near ambient) temperatures. This was therefore attributed to a great decrease of the activation energy of the benzene oxidations by lattice oxygens, with the reduced TiO_2 being reoxidized by gas-phase O_2. The photocatalytic oxidations of benzene over ZnO and titanate and the photocatalytic oxidations of acetaldehyde over WO_3 and TiO_2 were also proposed to happen in this way at elevated temperatures.[14−17] It has been also suggested that the photocatalytic oxidations over TiO_2, including 2-propanol-to-acetone,[18] methanol-(ethanol)-to-aldehyde,[19] and alcohol oxidations,[20] could take place apparently by using lattice oxygen of TiO_2 at room temperatures, with the gas-phase O_2 replacing reacted lattice oxygens. The universal character of the Mars–van Krevelen (MvK) pathway includes the participation of the catalyst's components in the reactions.[21−23] For organic oxidations over oxides, the MvK mechanism requires that lattice oxygens are first extracted and react with organics, with the generated oxygen vacancies being then replenished by gas-phase O_2 or other oxidative species.[24,25] Therefore, these studies meant that

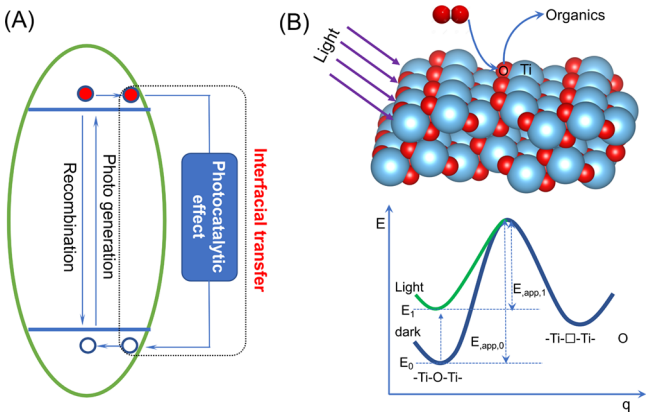

Figure 1. Mechanism of the photocatalysis driven by (A) charge carrier transfer mechanism and the photocatalysis happening according to (B) the light-assisted MvK mechanism. The charge carrier transfer driven photocatalysis requires that the photogenerated electrons go out of a semiconductor by an interfacial transfer way and then go back to the semiconductor after causing the photocatalytic effect. Instead, in the light-assisted MvK mechanism, light illumination reduces the thermal barrier for extracting lattice oxygens.

the photocatalytic oxidations of organics might happen via the redox cycle of the MvK pathway.[12−20]

Because this pathway also requires UV light excitation of electrons from the CB to VB, it is called the light-assisted MvK mechanism in this research. Based on the above description, the mechanism of the light-assisted MvK pathway is shown in Figure 1B. In this pathway, the role of light excitation is to reduce the thermal barrier of lattice oxygens reacting with organics;[12] this would lead to an increase in oxidations happening via the MvK pathway, apparently showing as a photocatalytic effect. Therefore, the intrinsic feature of the light-assisted MvK pathway in organic oxidations over oxides involves a light-assisted extraction of lattice oxygens to react with organics. Because the light-assisted lattice oxygen extraction might be not sensitive to heat activation, for example, direct light reduction of oxides, the light-assisted MvK mechanism does not mean a pure light-assisted increase of the thermocatalytic effect.

It is important to note that the charge carrier transfer pathway might happen via the MvK redox cycle. After trapping photoinduced holes, it was proposed that the lattice oxygens of TiO_2 can also participate in organic oxidations, and the generated oxygen vacancies are then replenished with O_2^- species.[20] It was also proposed that the benzene molecule (C_6H_6) could first trapped a hole to be transferred as active benzene ($C_6H_6^+$), which can then react with lattice oxygens of TiO_2, and the reduced TiO_2 was reoxidized by O_2^-.[13] Therefore, the charge carrier transfer and the MvK pathways cannot be rigorously distinguished in the case that the photoinduced charge carriers participate in photocatalytic oxidations along with lattice oxygens. In addition, it seems that whether photocatalysis could happen via the MvK pathway might depend on temperatures. For example, it was suggested that the photocatalytic oxidations of benzene over TiO_2 followed the charge carrier transfer pathway at ambient temperature, which would transfer to the light-assisted MvK pathway at elevated temperatures, for example, 240 or 290 °C.[12,13]

Taking TiO_2 as an example, although it has been seen that lattice oxygens might be extracted by organics under anaerobic conditions upon light illumination, many isotopic labeling studies also revealed that photocatalytic oxidations of organics generally do not need participation of lattice oxygens under aerobic conditions due to the presence of other oxidative radicals caused by charge carrier transfer (see subsection 3.2.3). This implies that photocatalytic oxidations might not proceed via the light-assisted MvK pathway when O_2 is present. Therefore, whether a photocatalytic oxidation could happen via the light-assisted MvK pathway seems to be dependent on organics to be oxidized, or there is still an inconsistency. Because light-assisted extraction of lattice oxygens from oxides plays a major role in this mechanism, we will discuss between the charge carrier transfer and the light-assisted extraction of lattice oxygens so as to disclose the importance of the light-assisted MvK pathway in a VOC photocatalysis under aerobic conditions.

TiO_2 was chosen because it is a typical photocatalyst that has been widely used in photocatalytic oxidations. Transient photocatalytic studies have already revealed that lattice oxygens could be extracted to oxidize formic acid under anaerobic conditions.[41] In addition, formic acid adsorbs on TiO_2 surfaces in a dissociated mode. The resulting formates and H ad-atoms can then be oxidized as CO_2 and H_2O upon light illumination without forming any long-lived intermediates and carbonate depositions.[26,27] Therefore, instead of other organics, this research therefore chose formic acid to be oxidized to obtain a more general conclusion. To have a good recognition, a comprehensive study, including apparent kinetics, online electric conductances, vacuum electric conductances, online optical transmittance, and first principle calculations, was carried out to discuss this problem. By combining the analysis of other published results, we obtained a result that the photocatalytic oxidation of formic acid in the presence O_2 should follow the charge carrier transfer pathway at both low and elevated temperatures, and the probability of the light-assisted MvK pathway should be very low.

2. EXPERIMENTAL SECTION

2.1. Materials. Commercial P25 TiO_2 (primary particle size of >25 nm, surface area of ∼50 m^2/g, anatase-to-rutile ratio of around 3:1) was used as the photocatalyst. Twenty milligrams of P25 was ultrasonically dispersed in a glass container (ϕ 50) with 5 mL of water. The water was then removed by heating at ∼100 °C for half an hour to form a thin TiO_2 coating on the bottom of the glass container. This thin TiO_2 coating was used for the photocatalysis of formic acid.

2.2. Photocatalytic Measurements. Photocatalytic and thermocatalytic experiments were done in a self-designed quartz closed-circulation cylindrical reactor (Figure S1). The main part of the reactor is a cylindrical quartz glass container and is linked with a Photoacoustic IR Multigas monitor (INNOVA Air Tech Instruments Model 1412) to monitor organic and CO_2 concentrations. A Pt100 resistance thermometer detector (RTD) connected with a temperature display was inserted into the reactor to check the real reaction temperature. A heating plate underneath was used to heat the reactor. The heating plate was adjusted until the reactor temperature reached the required value as detected by a Pt100 RTD. A mercury lamp (USHIO SP-9), with light output with a thin optical fiber, was used as the light source. A band-passed optical filter was used to generate 365 nm monochromic light. The light intensity reaching the TiO_2 surface was determined with a Si diode photodetector. For temperature-variable

experiments, the temperature was changed between 20 and 215 °C with 15 °C intervals at constant light intensity (3 mW/cm^2). For light intensity-variable experiments, the light intensity was changed at a constant temperature. The effect of light illumination on surface temperature was confirmed by infrared thermography (FLIR E60), which showed that the light illumination did not cause a change in surface temperature.

Carbon dioxide (CO_2) evolution was used to evaluate the photocatalytic activity. Because carbonate contaminations on a TiO_2 surface can also contribute to the CO_2 generation, all samples were first preilluminated by UV light for 24 h to remove carbonate contamination before starting the experiments. Fresh air was then flowed through the reactor for ∼15 min to purge out the old air until the initial CO_2 concentration was lower than 20 ppm. The reactor tightness was also confirmed to be good by observing a change in CO_2 concentration in a blank experiment.

Two experiments were designed for photocatalytic and thermocatalytic experiments according to the following procedures, as shown in Figure S2. Before injecting formic acid, the reactor was first kept in the dark for 30 min at the set temperature, and then light was switched on to illuminate the TiO_2 sample for another 30 min to see the effect of carbon contaminations. By switching off the lights, 2 μL of liquid formic acid was then injected into the reactor to observe a pure thermocatalytic effect in procedure 1 (Figure S2A). Differently, as shown in Figure S2B, by keeping the light on, 2 μL of liquid formic acid was injected to observe the photocatalytic effect in addition to the thermocatalytic effect in procedure 2. The pure photocatalytic effect was obtained by subtracting the CO_2 evolution speeds of procedure 2 with that of procedure 1. The photocatalytic rates were evaluated by using the initial CO_2 evolution speeds, as shown in Figure S2A,B.

2.3. Electric Conductance Measurement. The electronic conductances over the course of the formic acid photocatalysis were measured with a self-designed reactor (Figure S3). The main part includes a steel cylinder container and a top cover containing a piece of quartz glass for light illumination. Two electrodes, which were connected with an electric source meter, were mounted on the wall of a cylinder container. A thin TiO_2 coating was prepared on a quartz glass substrate by doctor-blading a p25 paste, which was then subjected to annealing at 450 °C for 1 h to remove organics. Two gold thin film electrodes were deposited on the TiO_2 coating to leave a 0.2 mm TiO_2 strip between them for conductance measurements (Figure S4). Additionally, two large-area TiO_2 coated quartz glasses were also placed in the reactor for photocatalytic reactions. A Pt100 RTD was sealed inside the reactor and connected to a temperature display to show the reaction temperature. A heat plate was used to heat the reactor to the required temperature. A solar simulator equipped with a band-passed filter is used to generate 365 nm monochromic light that does not lead to an increase in surface temperature. The conductances were measured at different light intensities by keeping the temperature unchanged and at different temperatures by keeping light intensity unchanged. The conductances were also measured in N_2, O_2, and air atmospheres with light intensity and temperature being kept unchanged. For each atmosphere, the corresponding gas (N_2, O_2, or air) was piped through the reactor for at least 3 h to drain out the old atmosphere. For all measurements, after injecting 2 μL of liquid formic acid, the reactor was kept in the dark for 10 min to allow evaporation. The UV light was turned on to illuminate the TiO_2 sample. The photocatalytic activity and the online conductances of the TiO_2 coating were monitored during the whole procedure with a Photoacoustic IR Multigas monitor (INNOVA Air Tech Instruments Model 1412) and an electronic source meter (KEITHLEY 2450 SourceMeter).

Vacuum conductances were measured in a self-designed setup that contains an electrical conductance measurement part, a vacuum system, an atmospheric system, a temperature-controlling system, and a light source, as shown in Figure S5. The INSPEC electrical conductance testing chamber containing a temperature-programmed sample platform is the main part. The top cover contains a piece of quartz glass to allow light illumination on the sample surface. The temperature can be under accurate control between −190 and 450 °C via a heating and a liquid N_2 cooling system. The TiO_2 coating and the Au film electrodes were prepared according to the same manner. After the TiO_2 coating was placed on the sample platform, the chamber was evacuated to below 1 m Torr by combining a mechanical pump and a molecular pump. The vacuum conductances at different temperatures and different O_2 partial pressures under simultaneous light illumination were measured. The UV light was generated according to the same way above. For both the air pressure and vacuum conductance measurements, the resistances were measured with a four-probe mode with 1.0 V voltage drop between the two Au electrodes.

2.4. UV−Vis Transmittance Spectroscopy. The online UV−vis transmittance spectra in the course of the photocatalytic degradation of formic acid under light illumination were measured by using a self-designed reactor (Figure S6) at ambient temperature. Before starting the measurement, high-purity N_2 was flowed through the reactor at least for 30 min to expel as much of the residual O_2 as possible. In the presence of formic acid (3 μL), the UV−vis transmittance spectra in the dark and under light illumination were measured to see the effect of light illumination on the UV−vis absorption, with the dark UV−vis spectrum being used as the baseline. To avoid the effect of incident light on the transmittance spectra measurement, a mercury lamp (USHIO SP-9) was equipped with a band-passed optical filter to allow the 365 nm monochromic light illumination on the sample. The light intensity approaching the sample surface was estimated to be around 1 mW/cm^2. Under simultaneous UV light illumination, the dynamic changes in optical absorption at 450 and 800 nm were measured to show the electronic structure induced by formic acid photocatalysis.

2.5. First Principle Calculation. The first principle computational calculation was performed by the DFT plane wave pseudo potential method. The general gradient approximation (GGA) with the Perdew−Burke−Ernzerhof (PBE) functional and ultrasoft pseudopotentials was used to describe the exchange correlation effects and electron ion interactions. The kinetic energetic cutoffs of 24 and 288 Ry for the smooth part of electronic wave functions and augmented electron density were used. The Quantum-ESPRESSO code, Pwscf package,[28] was used to perform the ab initio quantum calculation. Monkhorst-Pack (M-P) *k*-space sampling was adopted for SCF calculations. The convergence threshold for the self-consistency energy calculation was set to 10^{-8} Ry.

The slab model was used to construct an anatase (101) surface. The surface was represented by three-layer slabs made

of 2 × 3 unit cells; this is enough to assess the influence of removing a surface bridging oxygen. A vacuum space (20 Å) of sufficient separation was imposed to ensure no interaction with the lowest layer of the upper slabs. In addition to the bridging oxygen (O_{br}), all other Ti and O atoms were fixed during the calculation. The bridging oxygen was replaced from one position to another position along the Z axis. The dependence of the total energy on the average Ti−O_b bond length was plotted to obtain a potential energy landscape.

3. RESULTS AND DISCUSSION

3.1. Apparent Kinetics of Formic Acid Photocatalytic Oxidations over TiO_2. The blank experiment showed that formic acid was not subjected to direct oxidation in the absence of TiO_2. However, the decrease in formic acid concentration was also seen due to an inevitable adsorption on reaction systems, although CO_2 was not generated. Therefore, CO_2 evolutions were used to show the rates of formic acid photocatalytic oxidations according to Figure S2. The rates of formic acid thermocatalytic and photocatalytic oxidations were obtained from the CO_2 evolutions at different temperatures in the dark and upon illumination (Figure S7).

The Arrhenius dependences of photocatalytic and thermocatalytic rates on temperatures are shown in Figure 2. TiO_2 presents obvious thermocatalytic activity when the temperature exceeds 125 °C. The photocatalytic effect (red line) was obtained by removing the thermocatalytic contribution (black line). The thermocatalysis is in good agreement with the thermal activation mode. The apparent activation energy (E_{app}) was determined to be 52.71 ± 4.21 kJ/mol (0.55 eV). The photocatalysis also follows an Arrhenius mode when the temperature was lower than 125 °C. Its E_{app} is 8.48 ± 1.17 kJ/mol (0.09 eV). This result indicates that the photocatalytic oxidation of formic acid should be dominated by a single mechanism at temperatures below 125 °C so no transition in the photocatalytic pathway could be determined. The decrease of photocatalytic activity at temperatures higher than 125 °C will be discussed below (see section 3.5). If the photocatalysis at ambient temperatures is dominated by charge carrier transfer, this result shows that the photocatalysis over all temperatures must be driven by charge carrier transfer.

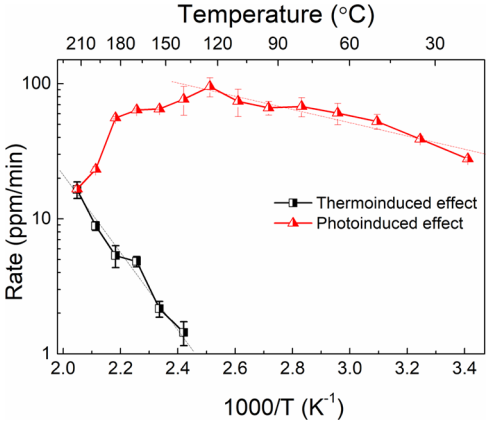

Figure 2. Arrhenius plots of thermocatalysis and photocatalysis of formic acids by TiO_2 under UV light illumination at different temperatures.

The photocatalytic rates reach maxima at 125 °C. We also studied the photocatalytic oxidations of formic acid by varying the light intensity at this temperature. Figure 3 shows the log−log dependence of the photocatalytic rate on light intensity (I).

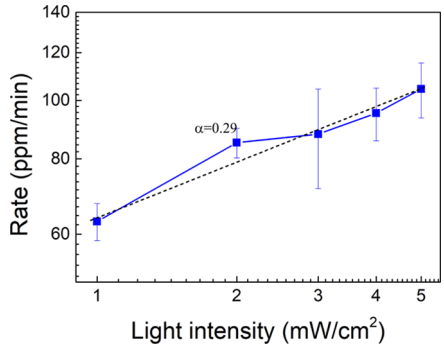

Figure 3. Log−log dependence of the speeds of the formic acid photocatalysis on light intensity.

It has already been revealed by many studies that, if a photocatalysis is driven by the charge carrier transfer, its speed depends on light intensity in a (sub)linear way according to $r \propto I^{\alpha}$, where I is the light intensity and α is the index.[29] It is seen from Figure 3 that the I-dependence of the formic acid photocatalysis on TiO_2 is in good agreement with a sublinear mode, and the index α is 0.29. Zhu et al. studied the formaldehyde photocatalysis over TiO_2 at some higher light intensity;[30] their results also showed that the formaldehyde photocatalysis depends on light intensity in a (sub)linear way. Therefore, the above result indicates that the photocatalytic oxidation of formic acid over TiO_2 should proceed according to the charge carrier transfer mechanism, rather than the light-assisted MvK mechanism; this will be discussed in detail below.

3.2. Unimportance of Light-Assisted Lattice O Heat Extraction in Photocatalytic Oxidation under Aerobic Conditions. The above study shows that the mechanism of formic acid photocatalysis over TiO_2 is the same over low and elevated temperatures. A transition from the charge carrier transfer to the light-assisted MvK mechanism was not identified. Here, we will discuss the light-assisted extraction of lattice oxygens from TiO_2 and its contribution to the photocatalytic effect by combining published results.

3.2.1. Lattice Oxygen Extraction by Direct Photoreduction. Different from dark conditions, lattice oxygen extraction includes three cases upon light illumination. First, lattice oxygens could be extracted under direct breaking of Ti−O bonds by light excitation, which is known as photoreduction. However, the quantum yield is very low. For example, it was shown by XPS that the quantum yield is 5.0×10^{-7}.[31] STM study also revealed that the cross section for forming oxygen defects by photoreduction is $10^{-23.5}$ cm^2 $photon^{-1}$.[32] Because the light fluxes used in these studies were almost two orders of magnitude higher than that used in usual photocatalysis, this kind of light-assisted lattice oxygen extraction might be statistically meaningless to a real photocatalytic oxidation.

3.2.2. Light-Assisted Heat Extraction of Lattice Oxygens. Lattice oxygens could be also extracted in the following way. Light excitation generates a h-polaron (O^-) in the TiO_2 lattice and elongates the Ti−O^- bond length.[33,34] As shown in Figure 4A, the Ti−O^- bond evolves on its own potential energy surface (PES), which returns by relaxation to its ground state PES, albeit with an excited vibrational energy. The oxidative reaction may take place when the excited vibration energy is

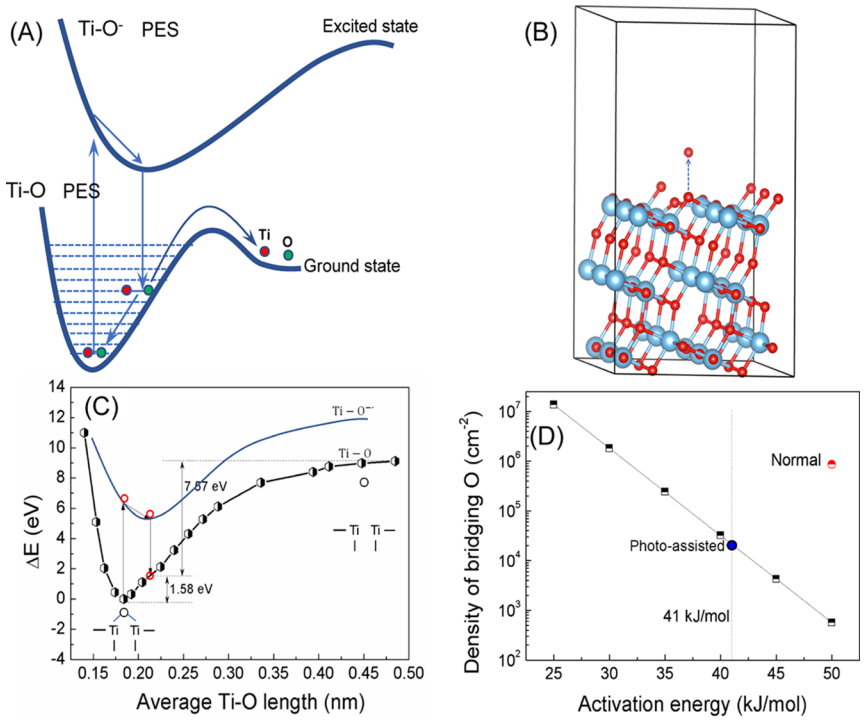

Figure 4. (A) Diagram potential energy landscape for the Ti−O bond and Ti−O− bond; (B) atomic slab model for anatase (101) surface, with an O_{br} being replaced from one position to another; (C) the potential energy landscape of anatase (101) surface by moving the Obr along Z direction; (D) dependence of activation speed of surface O_{br} via light-assisted heat extraction and the activation speed of surface O_{br} via the normal heat extraction.

sufficient to overcome the energy barrier for releasing an active oxygen atom. This description of light-assisted lattice oxygen extraction does not involve the transient leaving of photo-induced holes from TiO_2 to reactive substrates. In this case, light illumination only reduces the thermal barrier for heat extraction of lattice oxygens by organics, so it means that photocatalysis is a pure light-assisted increase of the thermocatalytic effect.

To show its importance, we theoretically compared the speed of this kind of lattice extraction with that of normal pure heat extraction. It has been shown that the Ti−O bond length could be elongated by ∼10% in forming an h-polaron (O^-).[35] By means of a first principle calculation, the PES of an anatase TiO_2 (101) surface was estimated by moving a bridging oxygen atom along the Z direction, as shown in Figure 4B. The dependence of total potential energy on the Ti−O_{br} (bridging oxygen) bond length is shown in Figure 4C. The dissociation energies of a Ti−O_{br} bond with a ground vibrational energy and a 10% elongated Ti−O_{br} bond with the excited vibrational energy are 9.15 and 7.57 eV, respectively. Therefore, the thermal barrier for extracting a vibrationally excited bridging oxygen atom from an anatase TiO_2 (101) surface is estimated to be more than 80% of that of Ti−O_{br} in the ground state.

It was reported that the thermal barrier of lattice oxygen extraction from TiO_2 by a methoxy group is ∼33 kJ in the dark.[36] Our results show that the energy barriers are 52 kJ/mol for formic acid thermocatalysis. The thermal energy barrier for benzene thermocatalysis is ∼56 kJ/mol.[12] Therefore, it is reasonable to assume that the energy barrier for extracting a lattice oxygen in thermocatalysis is ∼50 kJ/mol, based on which we gave an estimation for the light-assisted lattice O activation and normal lattice oxygen thermal activation (see the Supporting Information). According to this calculated PES and experimental data, the energy barrier for the light-assisted heat extraction of lattice oxygens from an anatase TiO_2 (101) surface was assumed to be ∼40 kJ/mol, much higher than the E_{app} of photocatalysis (∼8.5 kJ/mol). As shown in Figure 4D, the rate of the light-assisted heat extraction of bridging lattice oxygens is at least two orders of magnitude lower than that of the normal heat extraction even at room temperature. Therefore, it was thought that this kind of extraction of lattice oxygens cannot play a leading role under normal conditions.

3.2.3. Heat Extraction of Lattice Oxygens Carrying Photoinduced Holes (O^- Species). Lattice oxygens could be also extracted along with the photogenerated holes. In this case, a photogenerated hole could be first trapped at a lattice oxygen; the resulting O^-, carrying the hole, has higher activity and can then be extracted to oxidize organics. The formed oxygen vacancy on the TiO_2 surface could be replenished by O_2 dissociation at a fast rate. Therefore, in principle, the photocatalysis happening in this way follows the light-assisted MvK mechanism. However, because the photogenerated holes also go out of semiconductors for participation in photo-catalysis along with lattice oxygens, the photocatalysis therefore also follows the charge carrier transfer pathway. In a broad sense, although this case could be thought as the light-assisted MvK pathway, it does not mean a photoassisted increase of the pure thermocatalytic effect.

Many works have studied this light-assisted lattice oxygen extraction and its role in TiO_2 photocatalysis under anaerobic conditions. Isotope experiments have shown that TiO_2 lattice oxygens could be extracted upon UV light irradiation;[37−39] this was reported to have contribution to the photocatalysis of formic acid, acetic acid, and benzene in the absence of O_2.[12,40,41] Direct participation of bridging lattice oxygens of TiO_2 in water photocatalysis and benzene aqueous photo-

catalysis was also proposed using $Ti^{18}O_2$ as a photocatalyst.[42,43] Furthermore, under anaerobic conditions, direct involvement of bridging lattice oxygens in gaseous acetaldehyde photocatalytic oxidation on the anatase surface was observed by isotopic studies.[44] Under an ultrahigh vacuum condition, the photoinduced extraction of lattice oxygens from TiO_2 by organics was also observed.[30] It has been reported that the transient photocatalytic oxidations of acetic acid and formic acid under anaerobic conditions also involved an extraction of lattice oxygens from TiO_2, with the oxygen diffusion from the bulk to the surface providing the oxygens needed for reacting with these organics.[40,45]

Under anaerobic conditions, this light-assisted extraction of lattice oxygens from TiO_2 for organic oxidations was not supported in some studies. For example, Ngo et al. attributed the photocatalysis of acetic acid over TiO_2 to hole mediation.[46] Some studies were compared between thermocatalysis and photocatalysis of methanol, acetaldehyde, acetic acid, and formaldehyde and also did not evidence the light-assisted extraction of lattice oxygens in photocatalysis due to their different reaction pathways.[47−51] It has been also reported that the residual O_2 molecules contribute to high-vacuum CO photocatalysis under electron transfer mediation, rather than the light-assisted lattice oxygen extraction.[52] Spectroscopic study has also shown that the light-assisted lattice oxygen extraction was unimportant in photocatalysis. For example, in situ high-vacuum IR study revealed that the photoinduced transformations of methoxy to formate agreed well with a two-hole-mediated mechanism.[36] Although some studies have reported the role of lattice bridging oxygens in the light-assisted organic species dissociation on a TiO_2 surface, they also did not claim the direct light-assisted extraction of lattice oxygens.[53,54]

Under aerobic conditions, ^{18}O isotope labeling study has revealed that the alcohol-selective photocatalysis on a TiO_2 surface does not involve the extraction of lattice oxygens but was directly transferred from molecular O_2.[55] Other photocatalytic reactions, including the cleavage of aryl rings and the decarboxylation of saturated carboxylic acids, did not involve the attendance of lattice oxygens.[56] An isotope labeling study has further revealed that both ^{18}O atoms in $H_2{}^{18}O$ and $^{18}O_2$ were directly transferred to react with benzene without the participation of lattice oxygens.[57] In addition, an FTIR study showed that the oxygen exchange between formates on TiO_2 and $^{18}O_2$ does not need the participation of lattice oxygens.[58] It has been also seen by an isotopic study that the photoelectrochemical oxidation of formic acid on O^{18}-enriched TiO_2 did not include the transfer of ^{18}O from TiO_2 to CO_2.[59] By using a pure $Ti^{18}O_2$ photocatalyst, by means of FTIR, an isotopic study has also been carried out to study the role of lattice oxygens in formic acid oxidation.[60] Although small amounts of $C^{16}O^{18}O$ and $C^{18}O_2$ were detected, they were not from the reaction between lattice ^{18}O with formates on the TiO_2 surfaces but from the O-exchange between the generated $C^{16}O_2$ and $Ti^{18}O_2$. A transient photocatalytic study shows that the acetic acid photocatalytic decomposition under anaerobic conditions might involve participation of lattice oxygens, while that under aerobic conditions unlikely follows the MvK mechanism, and the adsorbed oxygen should react with acetic acid in a different pathway.[45]

Therefore, it can be known that this kind of lattice oxygen of TiO_2 might be extracted upon light illumination to participate in photocatalytic reactions under anaerobic condition due to the absence of other oxygen species. However, it should be unimportant under aerobic conditions because other pathways, caused by charge carrier transfer, could play a major role in photocatalytic oxidations of formic acid over TiO_2 materials.

3.3. Confirmation of the Charge Carrier Transfer Mechanism. Online electrical conductance experiments were carried out to confirm that the photocatalytic oxidations of formic acid over TiO_2 result from charge carrier transfer in an air atmosphere. In the light-assisted MvK mechanism, the light-assisted extraction of lattice oxygens in general is the limiting step of TiO_2 photocatalysis. This mechanism creates oxygen vacancies on a TiO_2 surface, which can then be replenished by O_2 in a faster speed.[61,62] Therefore, TiO_2 cannot be reduced in air for low-level organic oxidation under normal light illumination if the photocatalysis happens in the light-assisted MvK mode. Because the TiO_2 does not present an electrical conductance in the absence of formic acid upon UV light illumination in air, it is expected that the online conductances also do not respond to UV light illumination if the photocatalysis happens in this way. On the contrary, the online conductances will present a sharp change due to the sudden change in the electron number if the photocatalysis results from charge carrier transfer.[63,64]

Figure 5A shows the photoconductances of TiO_2 and CO_2 evolutions during the photocatalytic oxidations of formic acid

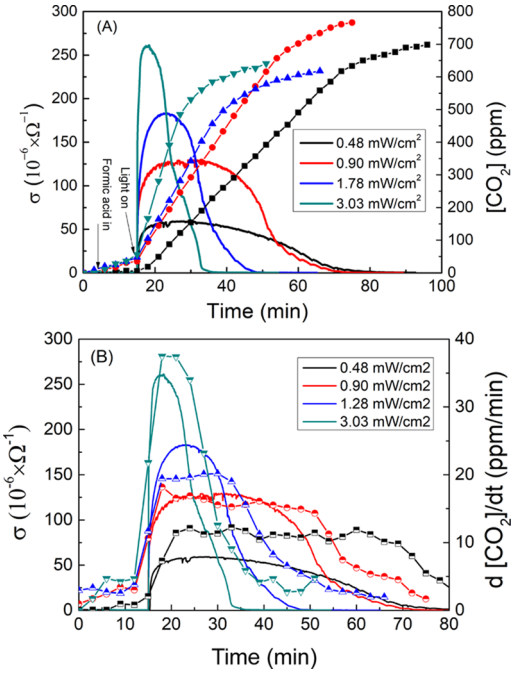

Figure 5. (A) Online electric conductances and corresponding CO_2 evolution in the course of formic acid photocatalysis under UV light illumination with different light intensities and at 60 °C; (B) comparison between the time dependences of the online photoconductances and $d[CO_2]/dt$.

at 30 °C in air for different light intensities. This shows a sharp increase in electrical conductances upon light illumination, along with a gradual CO_2 evolution. The conductances are determined by the electron injection from formates to TiO_2 and electron transfer from TiO_2 to O_2. Because the O_2 concentration does not change in the course of the photocatalysis, the conductance profiles should match the rate of CO_2 evolution to some extent. Figure 5B shows that the

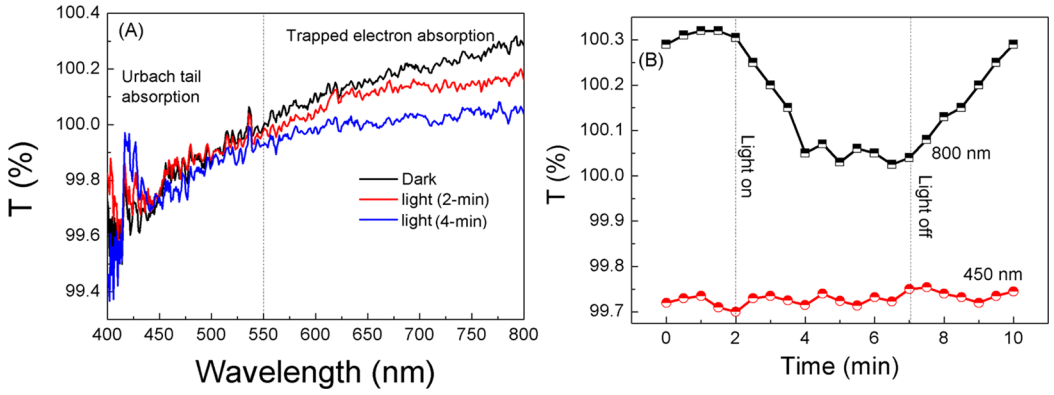

Figure 6. (A) Room temperature UV−vis spectroscopic transmittance of a P25-TiO_2 coating in the dark and under UV light illumination; (B) dynamic change in absorption at 450 and 800 nm in the course of formic acid photocatalysis under UV light illumination. (Note that sample transmittance in the dark was used for the baseline for measuring the change induced by light illumination. We thought that the transmittance slightly higher than 100% is due to the system mistake and instability during the measurement.)

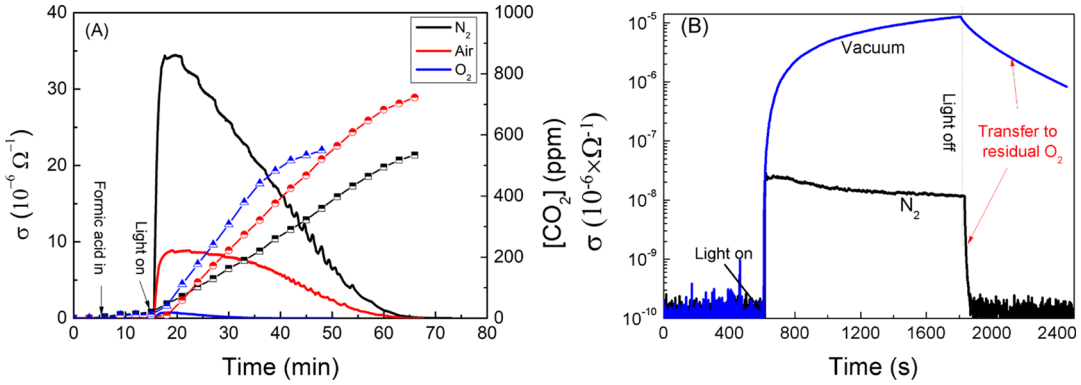

Figure 7. (A) Online conductances and corresponding CO_2 evolution in the course of formic acid photocatalysis in N_2, air and O_2 at 30 °C under 0.6 mW/cm^2 light illumination; (B) comparison between the photoconductances of TiO_2 material in N_2 atmosphere and vacuum (temperature: 30 °C; light intensity: 1.0 mW/cm^2).

conductance profiles and d[CO_2]/dt present such a matching to some extent, implying that the photoconductances result from charge carrier transfer, rather than a lattice oxygen extraction, hence supporting the conclusion that the formic acid photocatalysis is driven by hole transfer.

Online UV−vis transmission spectra of TiO_2 coating were further measured to monitor any dynamic change of the TiO_2 electronic structure during the photocatalytic oxidation of formic acid under N_2 protection. Oxygen vacancies in general relate with the Urbach tail absorption of TiO_2, so it is expected that the light-assisted extraction of lattice oxygens will lead to an increase in the exponential tail absorption below the absorption edge.[65] However, the light-induced injection of electrons to TiO_2 mainly leads to a change in near-IR absorption, arising from trapped electrons.[66] Figure 6A shows the UV−vis transmittance spectra of the TiO_2 coating before and after UV light illumination in the presence of formic acid after correcting for the baseline related to the dark transmittance of the TiO_2 coating. Dynamic changes in transmittances at 450 nm (oxygen vacancies) and 800 nm (trapped electrons) were monitored, as shown in Figure 6B. It is seen that the Urbach tail absorption associated with oxygen vacancy generation is unchanged because the transmittance below 550 nm is unchanged, whereas the absorption relating to trapped electrons shows an increase because the transmittance above 500 nm shows a regular decrease. This result shows that the electron generation in TiO_2 does not correlate with oxygen vacancy formation, agreeing well with the above online conductance analysis. In conclusion, the light-assisted extraction of lattice oxygens could not have a statistical meaning in the formic acid photocatalysis; this is also in agreement with the above first principle calculation.

3.4. Effect of Residual O_2 in an Inert Atmosphere. The photocatalytic oxidations of organics by TiO_2 in principle are lower under anaerobic conditions.[41] In the absence of O_2, the lattice oxygens on the TiO_2 surface are extracted to react with organics upon UV light illumination, which are then replenished by the oxygens diffusing from the bulk. The diffusion of lattice O from the bulk to the surface was thought to limit the anaerobic photocatalysis.[41,42] The oxygen diffusion from the bulk to the surface for healing oxygen vacancies has been studied by high-resolution dynamic STM on a single-crystalline anatase TiO_2 (101) surface.[67] The thermal barrier of this diffusion was estimated to be between 0.6 and 1.2 eV, much higher than the E_{app} of the formic acid photocatalytic oxidations (~0.09 eV). Therefore, the mechanism of aerobic photocatalysis of formic acid over TiO_2 is different from which happens under anaerobic conditions.

However, it was reported that photocatalytic oxidations of benzene in the absence of O_2 had the E_{app} the same as that in the presence of O_2, based on which it was concluded that the photocatalytic oxidation of benzene in the presence of O_2 happened via the light-assisted MvK pathway.[12] The E_{app} was determined to be ~21 kJ/mol, also much lower that of oxygen

bulk-to-surface diffusion. Therefore, oxygen sources other than lattice oxygens might contribute to the benzene photocatalytic oxidation in an inert atmosphere. TiO_2 belongs to an n-type oxide favoring chemisorption of O_2, which cannot be removed by simply replacing an air atmosphere by adding inert gas. In addition, it is also impossible to remove all O_2 if O_2 was simply replaced by adding inert gas in a batch reactor. The residual O_2 in an inert atmosphere might also contribute to the photocatalysis. The online conductances during the formic acid photocatalysis were measured under a N_2 atmosphere and were compared with those in air and O_2 atmospheres. Figure 7A shows the online conductances and CO_2 evolutions. The electrical conductance is the highest in N_2, then air, and then O_2, and the rate of CO_2 evolution also shows an increase. The time profiles of online conductance should resemble that of CO_2 evolution if lattice oxygens are extracted to oxidize formic acids in N_2 due to a gradual reduction of TiO_2. However, the electrical conductance presents a sharp increase to a maximum and then decreases, completely different from the continuous CO_2 evolution. This result shows that the photocatalytic oxidations of formic acid cannot be dominated by lattice oxygen extraction in N_2 protection. Because the conductance profiles are similar for the three atmospheres, the pathway of formic acid photocatalysis in N_2 must be the same as that in air and O_2. The first step is the fast injection of electrons from formic acid to TiO_2, and then the residual O_2, rather than the lattice oxygens, contributes to formic acid oxidation.

In the absence of formic acid, the electrical conductances in N_2 and in vacuum (the residual O_2 pressure is lower than 1.0×10^{-2} Pa) were compared to show the effect of residual O_2 in a N_2 atmosphere, as shown in Figure 7B. After stopping light illumination, because the decays of photoconductances are mainly attributed to the electron transfer to O_2 (see below), they clearly reveal that the residual O_2 in N_2 is much higher than that in vacuum and results in a photoconductance of approximately three orders of magnitude lower than that in vacuum. Therefore, simply adding an inert atmosphere into a batch reactor cannot eliminate the effect of O_2, which could indeed have an important effect on photocatalysis. As shown in Figure 6A, more electrons are accumulated in TiO_2 to obtain a high photocatalytic rate. Therefore, the simple attribution of photocatalytic oxidations in an inert atmosphere to the light-assisted extraction of lattice oxygens is unfounded if the effect of residual O_2 cannot be ruled out. The UV−vis spectra and Ti 2p valence states of TiO_2 materials before and after the formic acid photocatalysis in N_2 are almost the same (Figures S8 and S9); this also does not reveal the light-assisted reduction of TiO_2 materials by formic acid. It is also highly possible that the residual O_2 led to the benzene photocatalytic oxidations in an inert atmosphere, so its E_{app} is the same as that in the presence O_2.[12]

3.5. Effect of Temperature on Charge Carrier Transfer. Figure 8A shows the vacuum conductances measured at different O_2 partial pressures; this shows a decrease with O_2 partial pressure. Figure 8B further shows that the conductance decay increases with O_2 partial pressures. This result reveals that the transfer of electrons from TiO_2 to O_2 is the dominant way to eliminate the electrons contributing to conductances, so the reduced conductances indicate a faster electron transfer to O_2. By keeping the O_2 partial pressure at 5 Pa, Figure 8C shows that an increase in temperature results in a decrease in photoconductances. Figure 8D further reveals that the electron transfer to O_2 is accelerated by an increase in temperature.

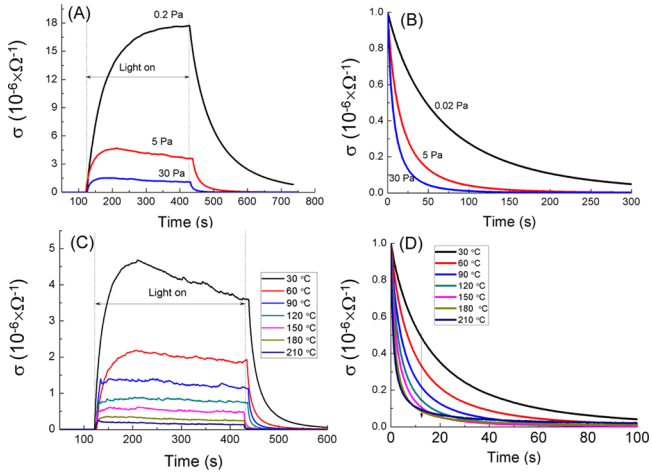

Figure 8. (A) Steady and transient electrical conductance of a P25-TiO_2 coating under different O_2 partial pressures at temperature of 30 °C; (B) normalized transient photoconductance at different O_2 partial pressures; (C) steady and transient electrical conductances of TiO_2 coating at different temperatures under the condition of 5 Pa oxygen partial pressure; (D) normalized transient photoconductances at different temperatures.

Although the decrease of photoconductances with temperatures is the same as that measured at atmospheric pressures,[12,13] our data leads to an opposite conclusion that the reduction in conductances with temperatures does not mean a decrease but a possible increase in the photocatalytic effect because the increase in electron transfer accelerates O_2 activation for organic oxidations. Therefore, this result provides a good proof that the photocatalytic effect, happening via the charge carrier transfer pathway, cannot be lowered by an increase in temperatures. To confirm this conclusion, the electrical conductances in the course of formic acid photocatalysis in air were also measured at different temperatures. Figure 9A shows that that the online photoconductances present an obvious decrease with temperature. However, instead of a decrease, CO_2 evolution speeds show a slight increase with temperature (Figure 2). These results confirm that the decrease in photoconductances with temperature can be ascribed to the increase of electron transfer to O_2 and that could then partially contribute to the increase in photocatalysis.

In addition, the vacuum conductances of TiO_2 with preadsorbed formic acid were also measured, as shown in Figure 9B. As compared to that without adsorbing formic acid, the conductance shows an increase due to electron injection from formic acid. Because electron transfer to O_2 is limited under vacuum conditions, this result shows that the formic acid photocatalysis is driven by hole transfer in its first step. It also confirmed that this hole-mediated process does not decrease with temperature, as a temperature rise can lead to an enhanced conductance. Therefore, we concluded that increasing temperatures can lead to an increase in both the electron and hole transfer. The result is in good line with the conclusion indicated in the apparent kinetic section, so the increase of photocatalytic activity with temperatures is the natural result of the increase of charge carrier transfer. The high photocatalytic activity at elevated temperatures is partially contributed to the normal role of heat in accelerating charge carrier transfer, which cannot be ascribed to the light-assisted increase due to a thermocatalytic effect. Therefore, the photocatalytic oxidations

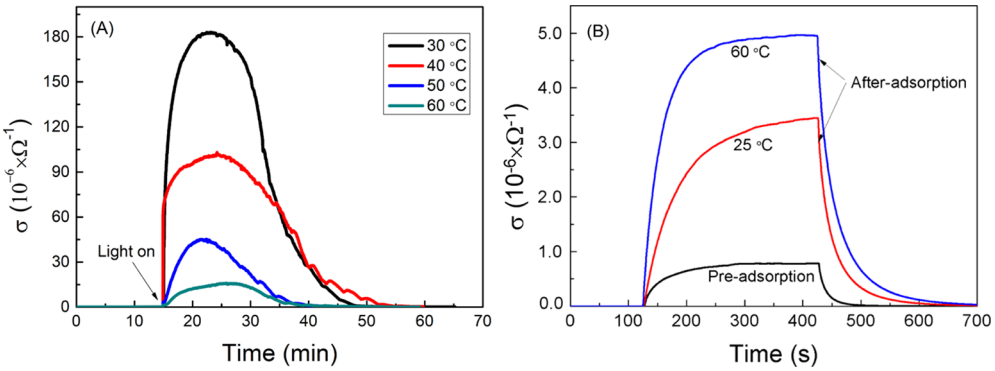

Figure 9. (A) Online photoconductances of TiO_2 coatings in the course of formic acid photocatalytic oxidations at different temperatures (light intensity: 1.8 mW/cm$_2$); (B) vacuum photoconductances of TiO_2 coatings before and after formic acid adsorption on TiO_2 surface (light intensity: 2.0 mW/cm^2).

of formic acid are dominantly driven by charge carrier transfer at both low and elevated temperatures. There is no transition from the charge carrier transfer to the light-assisted MvK mechanism when the temperature increases.

3.6. Heat-Induced Decrease of Photocatalytic Effect. Our data also points to the fact that the formic acid photocatalysis over TiO_2 tends to decrease when the temperature is higher than 125 °C. This heat-induced decrease effect in photocatalytic activity seems to be common because it was also seen by others. For example, it has been reported that the activity of ethylene photocatalysis tends to decrease at high temperatures.[68,69] A heat induced decrease of ethylene photocatalysis was experimentally observed when the temperature was higher than 130 °C.[70] A heat-induced decrease of photocatalysis of acetaldehyde was also observed when the temperature was higher than 130 °C.[71] It has been also reported that the benzene photocatalysis showed a heat-induced decrease when the temperature was higher than 200 °C.[72] In these studies, the heat-induced decrease in photocatalytic activity was ascribed to various reasons that included heat-induced organic desorption, multiphonon recombination, the removal of surface hydroxyls, and the others. We did not see a sudden increase in organic desorption around the transition temperature. It is also unlikely for surface dehydration to happen at the temperature around 120 °C.[73] It has been reported that chemically adsorbed O_2 molecules on TiO_2 surfaces desorb at temperatures above 120 °C.[74] Therefore, it is considered that the heat-induced decreased effect of photocatalysis can be possibly attributed to a O_2 thermal desorption from TiO_2 surfaces. Because the electron transfer to O_2 is an indispensable step to the photocatalytic cycle, the heat-induced decrease of photocatalytic activity at high temperature should be a common phenomenon in semiconductor photocatalysis.

4. CONCLUSIONS

In summary, the result of apparent kinetic analysis showed that there is no transition in the mechanism of the formic acid photocatalysis over TiO_2 with an increase in temperature. The combination of the first principle calculation, online electric conductances, and online optical transmittances revealed that the light-assisted extraction of lattice oxygens could not play a major role in the photocatalytic oxidation of formic acid in the presence of O_2, as compared to the charge carrier transfer pathway. The vacuum electric conductances further showed that the transfers of both the electrons and holes increase with temperature, so we concluded that the increase of the photocatalytic rate with temperature is due to the normal thermal activation in photocatalysis, not from a promotion by the light-assisted MvK pathway. In contrast, we also saw a heat-induced decrease in photocatalysis possibly due to the desorption of chemically adsorbed O_2. Therefore, a conclusion was obtained that the photocatalytic oxidations of formic acid over TiO_2 should follow the charge carrier transfer pathway at both low and elevated temperatures. The light-assisted extraction of lattice oxygens should be unimportant in the formic acid photocatalysis in the presence of O_2. Based on our results, we would like to note that it might be improper to attribute the higher activity of aerobic photocatalytic oxidations at elevated temperatures to a transition from the charge carrier transfer to the light-assisted MvK pathways, because the photocatalytic effect happening via the charge carrier transfer pathway increased with temperatures. Therefore, our results supported the conclusion that the higher photocatalytic rate at elevated temperatures should be attributed to the natural increase of charge carrier transfer. In addition, it was also important to note that great care must be taken to consider the effect of residual O_2 in an inert atmosphere if this was used to confirm the participation of lattice oxygens in photocatalysis.

■ ASSOCIATED CONTENT

Additional supporting figures showing description of photocatalytic experimental setup, diagram for evaluating photocatalytic rates, description for measuring online air pressure conductances, sample image for conductance measurement, description for measuring vacuum conductance measurement, description for measuring in situ optical transmittance, CO_2 evolutions during formic oxidations upon UV light illumination and in the dark, UV−visible transmittance spectra of TiO_2 coating before and after photocatalytic reaction, Ti 2p core-level XPS spectra of TiO_2 before and after photocatalytic reaction, and explanation for estimating the light-assisted and normal heat extraction of lattice oxygens (PDF)

AUTHOR INFORMATION

Corresponding Author

*E-mail: liubaoshun@126.com. Tel: +86-027-87669729.

ORCID

Baoshun Liu: 0000-0001-5564-3685

Notes

The authors declare no competing financial interest.

ACKNOWLEDGMENTS

B.L. thanks the National Natural Science Foundation of China (nos. 51772230 and 51461135004), National Key Research and Development Plan (2017YFE0192600), Hubei Foreign Science and Technology cooperation project (2017AHB059), and then Japan Society for the Promotion of Science (JSPS) for an Invitation Fellowship for Foreign Researchers (L16531). I.P.P. thanks the Wuhan University of Technology for a visiting professorship.

REFERENCES

(1) Zheng, Y.; Wang, W.; Jiang, D.; Zhang, L.; Li, X.; Wang, Z. Insights into the Solar Light Driven Thermocatalytic Oxidation of VOCs Over Tunnel Structured Manganese Oxides. *Phys. Chem. Chem. Phys.* **2016**, *18*, 18180−18186.

(2) Su, L.; Ye, X.; Meng, S.; Fu, X.; Chen, S. Effect of Different Solvent on the Photocatalytic Activity of $ZnIn_2S_4$ for Selective Oxidation of Aromatic Alcohols to Aromatic Aldehydes under Visible Light Irradiation. *Appl. Surf. Sci.* **2016**, *384*, 161−174.

(3) Chen, J.; Li, Y.; Fang, S.; Yang, Y.; Zhao, X. UV−Vis-Infrared Light-Driven Thermocatalytic Abatement of Benzene on Fe Doped OMS-2 Nanorods Enhanced by a Novel Photoactivation. *Chem. Eng. J.* **2018**, *332*, 205−215.

(4) Jin, Z.; Murakami, N.; Tsubota, T.; Ohno, T. Complete Oxidation of Acetaldehyde over a Composite Photocatalyst of Graphitic Carbon Nitride and Tungsten(VI) Oxide Under Visible-light Irradiation. *Appl. Catal., B* **2014**, *150-151*, 479−485.

(5) Uddin, M. T.; Babot, O.; Thomas, L.; Olivier, C.; Redaelli, M.; D'Arienzo, M.; Morazzoni, F.; Jaegermann, W.; Rockstroh, N.; Junge, H.; Toupance, T. New Insights into the Photocatalytic Properties of RuO_2/TiO_2 Mesoporous Heterostructures for Hydrogen Production and Organic Pollutant Photodecomposition. *J. Phys. Chem. C* **2015**, *119*, 7006−7015.

(6) Liu, B.; Cheng, K.; Nie, S.; Zhao, X.; Yu, H.; Yu, J.; Fujishima, A.; Nakata, K. Ice−Water Quenching Induced Ti^{3+} Self-doped TiO_2 with Surface Lattice Distortion and the Increased Photocatalytic Activity. *J. Phys. Chem. C* **2017**, *121*, 19836−19848.

(7) Petrik, N. G.; Kimmel, G. A. Electron- and Hole-Mediated Reactions in UV-Irradiated O_2 Adsorbed on Reduced Rutile TiO_2(110). *J. Phys. Chem. C* **2010**, *115*, 152−164.

(8) Petrik, N. G.; Kimmel, G. A. Photoinduced Dissociation of O_2 on Rutile TiO_2(110). *J. Phys. Chem. Lett.* **2010**, *1*, 1758−1762.

(9) Nosaka, Y.; Nosaka, A. Y. Generation and Detection of Reactive Oxygen Species in Photocatalysis. *Chem. Rev.* **2017**, *117*, 11302−11336.

(10) Liu, B.; Zhao, X.; Terashima, C.; Fujishima, A.; Nakata, K. Thermodynamic and Kinetic Analysis of Heterogeneous Photocatalysis for Semiconductor Systems. *Phys. Chem. Chem. Phys.* **2014**, *16*, 8751−8760.

(11) Turchi, C. S.; Ollis, D. F. Photocatalytic Degradation of Organic Water Contaminants: Mechanisms Involving Hydroxyl Radical Attack. *J. Catal.* **1990**, *122*, 178−192.

(12) Li, Y.; Huang, J.; Peng, T.; Xu, J.; Zhao, X. Photothermocatalytic Synergetic Effect Leads to High Efficient Detoxification of Benzene on TiO_2 and Pt/TiO_2 Nanocomposite. *ChemCatChem* **2010**, *2*, 1082−1087.

(13) Ren, L.; Mao, M.; Li, Y.; Lan, L.; Zhang, Z.; Zhao, X. Novel Photothermocatalytic Synergetic Effect Leads to High Catalytic Activity and Excellent Durability of Anatase TiO_2 Nanosheets with Dominant {001} Facets for Benzene Abatement. *Appl. Catal., B* **2016**, *198*, 303−310.

(14) Xie, W.; Li, Y.; Shi, W.; Zhao, L.; Zhao, X.; Fang, P.; Zheng, F.; Wang, S. Novel Effect of Significant Enhancement of Gas-Phase Photocatalytic Efficiency for Nano ZnO. *Chem. Eng. J.* **2012**, *213*, 218−224.

(15) Peng, X.; Wang, C.; Li, Y.; Ma, H.; Yu, F.; Che, G.; Yan, J.; Zhang, X.; Liu, Y. Revisiting Cocatalyst/TiO_2 Photocatalyst in Blue Light Photothermalcatalysis. *Catal. Today* **2019**, 286.

(16) Liu, Y.; Shu, W.; Chen, K.; Peng, Z.; Chen, W. Enhanced Photothermocatalytic Synergetic Activity Toward Gaseous Benzene for Mo+C-Codoped Titanate Nanobelts. *ACS Catal.* **2012**, *2*, 2557−2565.

(17) Li, Y.; Wang, C.; Zheng, H.; Wan, F.; Yu, F.; Zhang, X.; Liu, Y. Surface Oxygen Vacancies on WO_3 Contributed to Enhanced Photothermosynergistic Effect. *Appl. Surf. Sci.* **2017**, *391*, 654−661.

(18) Larson, S. A.; Widegren, J. A.; Falconer, J. L. Transient Studies of 2-Propanol Photocatalytic Oxidation on Titania. *J. Catal.* **1995**, *157*, 611−625.

(19) Cunningham, J.; Meriaudeau, P. Interactions of Butyl Alcohols with Flash-illuminated Rutile Surfaces. *J. Chem. Soc., Faraday Trans.1* **1976**, *72*, 1499.

(20) Walker, A.; Formenti, M.; Meriaudeau, P.; Teichner, S. J. Heterogeneous Photocatalysis: Photo-oxidation of Methylbutanols. *J. Catal.* **1977**, *50*, 237.

(21) Kröger, C. Zur Heterogenen Katalyse Binirer Gasreaktionen. II. *Z. Anorg. Chem.* **1932**, *206*, 289.

(22) Mars, P.; Van Krevelen, D. W. Oxidations Carried out by Means of Vanadium Oxide Catalysts. *Chem. Eng. Sci.* **1954**, *3*, 41−59.

(23) Doornkamp, C.; Ponec, V. The Universal Character of the Mars and Van Krevelen Mechanism. *J. Mol. Catal. A: Chem.* **2000**, *162*, 19−32.

(24) Stoyanova, M.; Konova, P.; Nikolov, P.; Naydenov, A.; Christoskova, S.; Mehandjiev, D. Alumina-supported Nickel Oxide for Ozone Decomposition and Catalytic Ozonation of CO and VOCs. *Chem. Eng. J.* **2006**, *122*, 41−46.

(25) Huang, H.; Xu, Y.; Feng, Q.; Leung, D. Y. C. Low temperature catalytic oxidation of volatile organic compounds: a review. *Catal. Sci. Technol.* **2015**, *5*, 2649−2669.

(26) Yang, J.; Liu, B.; Xie, H.; Zhao, X.; Terashima, C.; Fujishima, A.; Nakata, K. In Situ Photoconductivity Kinetic Study of Nano-TiO_2 during the Photocatalytic Oxidation of Formic Acid: Effects of New Recombination and Current Doubling. *J. Phys. Chem. C* **2015**, *119*, 21711−21722.

(27) Miller, K. L.; Falconer, J. L.; Medlin, J. W. Effect of Water on the Adsorbed Structure of Formic Acid on TiO_2 Anatase (1 0 1). *J. Catal.* **2011**, *278*, 321−328.

(28) Quantum ESPRESSO. http://www.quantum-espresso.org/.

(29) Salvador, P. Semiconductors' Photoelectrochemistry: A Kinetic and Thermodynamic Analysis in the Light of Equilibrium and Nonequilibrium Models. *J. Phys. Chem. B* **2001**, *105*, 6128−6141.

(30) Zhu, X.; Chang, D.-L.; Li, X.-S.; Sun, Z.-G.; Deng, X.-Q.; Zhu, A.-M. Inherent Rate Constants and Humidity Impact Factors of Anatase TiO_2 Film in Photocatalytic Removal of Formaldehyde from Air. *Chem. Eng. J.* **2015**, *279*, 897−903.

(31) Shultz, A. N.; Jang, W.; Hetherington, W. M., III; Baer, D. R.; Wang, L.-Q.; Engelhard, M. H. Comparative Second Harmonic Generation and X-ray Photoelectron Spectroscopy Studies of the UV Creation and O_2 Healing of Ti^{3+} Defects on (110) Rutile TiO_2 Surfaces. *Surf. Sci.* **1995**, *339*, 114−124.

(32) Mezhenny, S.; Maksymovych, P.; Thompson, T. L.; Diwald, O.; Stahl, D.; Walck, S. D.; Yates, J. T., Jr. STM studies of Defect Production on the TiO_2(110)-(1×1) and TiO_2 (110)-(1×2) Surfaces Induced by UV Irradiation. *Chem. Phys. Lett.* **2003**, *369*, 152−158.

(33) Deskins, N. A.; Dupuis, M. Electron Transport via Polaron Hopping in Bulk TiO_2: A Density Functional Theory Characterization. *Phys. Rev. B* **2007**, *75*, 195212.

(34) Zawadzki, P.; Laursen, A. B.; Jacobsen, K. W.; Dahl, S.; Rossmeisl, J. Oxidative Trends of TiO_2-hole Trapping at Anatase and Rutile surfaces. *Energy Environ. Sci.* **2012**, *5*, 9866−9869.
(35) Di Valentin, C.; Selloni, A. Bulk and Surface Polarons in Photoexcited Anatase TiO_2. *J. Phys. Chem. Lett.* **2011**, *2*, 2223−2228.
(36) Panayotov, D. A.; Burrows, S. P.; Morris, J. R. Photooxidation Mechanism of Methanol on Rutile TiO_2 Nanoparticles. *J. Phys. Chem. C* **2012**, *116*, 6623−6635.
(37) Civiş, S.; Ferus, M.; Zukalová, M.; Zukal, A.; Kavan, L.; Jordan, K. D.; Sorescu, D. C. Oxygen Atom Exchange between Gaseous CO_2 and TiO_2 Nanoclusters. *J. Phys. Chem. C* **2015**, *119*, 3605−3612.
(38) Sato, S.; Kadowaki, T.; Yamaguti, K. Photocatalytic Oxygen Isotopic Exchange between Oxygen Molecule and the Lattice Oxygen of titanium dioxide Prepared from Titanium Hydroxide. *J. Phys. Chem.* **1984**, *88*, 2930−2931.
(39) Mikhaylov, R. V.; Glazkova, N. I.; Nikitin, K. V. Photo-stimulated Oxygen Isotope Exchange between $N^{18}O$ and Anatase TiO_2 under Light Irradiation. *J. Photochem. Photobiol., A* **2017**, *332*, 554−561.
(40) Muggli, D. S.; Falconer, J. L. Role of Lattice Oxygen in Photocatalytic Oxidation on TiO_2. *J. Catal.* **2000**, *191*, 318−325.
(41) Muggli, D. S.; Keyser, S. A.; Falconer, J. L. Photocatalytic Decomposition of Acetic Acid on TiO_2. *Catal. Lett.* **1998**, *55*, 129−132.
(42) Panayotov, D.A.; Morris, J. R. Thermal Decomposition of a Chemical Warfare Agent Simulant (DMMP) on TiO_2: Adsorbate Reactions with Lattice Oxygen as Studied by Infrared Spectroscopy. *J. Phys. Chem. C* **2009**, *113*, 15684−15691.
(43) Montoya, J. F.; Bahnemann, D. W.; Salvador, P.; Peral, J. Catalytic Role of Bridging Oxygens in TiO_2 Liquid Phase Photocatalytic Reactions: Analysis of $H_2{}^{16}O$ Photooxidation on Labeled $Ti^{18}O_2$. *Catal. Sci. Technol.* **2017**, *7*, 902−910.
(44) Melchers, S.; Schneider, J.; Bahnemann, D. W. Isotopic Studies on the Degradation of Acetaldehyde on Anatase Surfaces. *Catal. Today* **2018**, DOI: 10.1016/j.cattod.2018.10.016.
(45) Muggli, D. S.; Falconer, J. L. Parallel Pathways for Photocatalytic Decomposition of Acetic Acid on TiO_2. *J. Catal.* **1999**, *187*, 230−237.
(46) Ngo, S.; Betts, L. M.; Dappozze, F.; Ponczek, M.; George, C.; Guillard, C. Kinetics and Mechanism of the Photocatalytic Degradation of Acetic Acid in Absence or Presence of O_2. *J. Photochem. Photobiol., A* **2017**, *339*, 80−88.
(47) Lin, Y.-C.; Chien, T.-E.; Li, K.-L.; Lin, J.-L. Comparison of the Thermal and Photochemical Reaction Pathways of Melamine on TiO_2. *J. Phys. Chem. C* **2015**, *119*, 8645−8651.
(48) Petrik, N. G.; Henderson, M. A.; Kimmel, G. A. Insights into Acetone Photochemistry on Rutile TiO_2(110). 1. Off-Normal CH_3 Ejection from Acetone Diolate. *J. Phys. Chem. C* **2015**, *119*, 12262−12272.
(49) Pepin, P. A.; Diroll, B. T.; Choi, H. J.; Murray, C. B.; Vohs, J. M. Thermal and Photochemical Reactions of Methanol, Acetaldehyde, and Acetic Acid on Brookite TiO_2 Nanorods. *J. Phys. Chem. C* **2017**, *121*, 11488−11498.
(50) Luo, B.; Tang, H.; Cheng, Z.; Ji, Y.; Cui, X.; Shi, Y.; Wang, B. Detecting the Photoactivity of Anatase TiO_2(001)-(1 × 4) Surface by Formaldehyde. *J. Phys. Chem. C* **2017**, *121*, 17289−17296.
(51) Cheng, Z.; Tang, H.; Cui, X.; Dong, S.; Ma, X.; Luo, B.; Tan, S.; Wang, B. Identifying the Site-Dependent Photoactivity of Anatase TiO_2(001)-(1×4) Surface. *J. Phys. Chem. C* **2017**, *121*, 19930−19937.
(52) Zhang, Z.; Yates, J. T., Jr. Electron-Mediated CO Oxidation on the TiO_2(110) Surface during Electronic Excitation. *J. Am. Chem. Soc.* **2010**, *132*, 12804−12807.
(53) Xu, C.; Yang, W.; Guo, Q.; Dai, D.; Yang, X. Photoinduced Decomposition of Acetaldehyde on a Reduced TiO_2(110) Surface: Involvement of Lattice Oxygen. *Phys. Chem. Chem. Phys.* **2016**, *18*, 30982−30989.
(54) Xu, C.; Yang, W.; Guo, Q.; Dai, D.; Minton, T. K.; Yang, X. Photoinduced Decomposition of Formaldehyde on a TiO_2(110) Surface, Assisted by Bridge-Bonded Oxygen Atoms. *J. Phys. Chem. Lett.* **2013**, *4*, 2668−2673.
(55) Zhang, M.; Wang, Q.; Chen, C.; Zang, L.; Ma, W.; Zhao, J. Oxygen Atom Transfer in the Photocatalytic Oxidation of Alcohols by TiO_2 : Oxygen Isotope Studies. *Angew. Chem., Int. Ed.* **2009**, *48*, 6081−6084.
(56) Pang, X.; Chen, C.; Ji, H.; Che, Y.; Ma, W.; Zhao, J. Unraveling the Photocatalytic Mechanisms on TiO_2 Surfaces Using the Oxygen-18 Isotopic Label Technique. *Molecules* **2014**, *19*, 16291−16311.
(57) Bui, T. D.; Kimura, A.; Ikeda, S.; Matsumura, M. Determination of Oxygen Sources for Oxidation of Benzene on TiO_2 Photocatalysts in Aqueous Solutions Containing Molecular Oxygen. *J. Am. Chem. Soc.* **2010**, *132*, 8453−8458.
(58) Liao, L.-F.; Lien, C.-F.; Shieh, D.-L.; Chen, M.-T.; Lin, J.-L. FTIR Study of Adsorption and Photoassisted Oxygen Isotopic Exchange of Carbon Monoxide, Carbon Dioxide, Carbonate, and Formate on TiO_2. *J. Phys. Chem. B* **2002**, *106*, 11240−11245.
(59) Bogdanoff, P.; Alonso-Vante, N. A Kinetic Approach of Competitive Photoelectrooxidation of HCOOH and H_2O on TiO_2 Anatase Thin Layers via On-Line Mass Detection. *J. Electroanal. Chem.* **1994**, *379*, 415−421.
(60) Civiş, S.; Ferus, M.; Zukalová, M.; Kubát, P.; Kavan, L. Photochemistry and Gas-Phase FTIR Spectroscopy of Formic Acid Interaction with Anatase $Ti^{18}O_2$ Nanoparticles. *J. Phys. Chem. C* **2012**, *116*, 11200−11205.
(61) Wendt, S.; Matthiesen, J.; Schaub, R.; Vestergaard, E. K.; Lægsgaard, E.; Besenbacher, F.; Hammer, B. Formation and Splitting of Paired Hydroxyl Groups on Reduced TiO_2 (110). *Phys. Rev. Lett.* **2006**, *96*, No. 066107.
(62) Setvín, M.; Aschauer, U.; Scheiber, P.; Li, Y.-F.; Hou, W.; Schmid, M.; Selloni, A.; Diebold, U. Reaction of O_2 with Sub-surface Oxygen Vacancies on TiO_2 Anatase (101). *Science* **2013**, *341*, 988−991.
(63) Herrmann, J. M.; Disdier, J.; Mozzanega, M.-N.; Pichat, P. Heterogeneous Photocatalysis: In Situ Photoconductivity Study of TiO_2 during Oxidation of Isobutane into Acetone. *J. Catal.* **1979**, *60*, 369−377.
(64) Disdier, J.; Herrmann, J.-M.; Pichat, P. Platinum/titanium dioxide catalysts. A Photoconductivity Study of Electron Transfer from the Ultraviolet-illuminated Support to the Metal and of the Influence of Hydrogen. *J. Chem. Soc., Faraday Trans. 1* **1983**, *79*, 651−660.
(65) Liu, B.; Zhao, X.; Yu, J.; Parkin, I. P.; Fujishima, A.; Nakata, K. Intrinsic Intermediate Gap States of TiO_2 Materials and Their Roles in Charge Carrier Kinetics. *J. Photochem. Photobiol., C* **2019**, *39*, 1−57.
(66) Huo, J.; Hu, Y.; Jiang, H.; Li, C. In-situ Surface Hydrogenation Synthesis of Ti^{3+} Self-doped TiO_2 with Enhanced Visible Light Photoactivity. *Nanoscale* **2014**, *6*, 9078−9084.
(67) Scheiber, P.; Fidler, M.; Dulub, O.; Schmid, M.; Diebold, U.; Hou, W.; Aschauer, U.; Selloni, A. (Sub)Surface Mobility of Oxygen Vacancies at the TiO_2 Anatase (101) Surface. *Phys. Rev. Lett.* **2012**, *109*, 136103.
(68) Obee, T. N.; Hay, S. O. Effects of Moisture and Temperature on the Photooxidation of Ethylene on Titania. *Environ. Sci. Technol.* **1997**, *31*, 2034−2038.
(69) Westrich, T. A.; Dahlberg, K. A.; Kaviany, M.; Schwank, J. W. High-Temperature Photocatalytic Ethylene Oxidation over TiO_2. *J. Phys. Chem. C* **2011**, *115*, 16537−16543.
(70) Yamazaki, S.; Tanaka, S.; Tsukamoto, H. Kinetic Studies of Oxidation of Ethylene over a TiO_2 Photocatalyst. *J. Photochem. Photobiol., A* **1999**, *121*, 55−61.
(71) Falconer, J. L.; Magrini-Bair, K. A. Photocatalytic and Thermal Catalytic Oxidation of Acetaldehyde on Pt/TiO_2. *J. Catal.* **1998**, *179*, 171−178.
(72) Lin, Y.; Wang, X.; Zeng, D. Effect of Temperature on Photocatalytic Performance of TiO_2 of TiO_2 nanotube. *Ceram. Int.* **2015**, *32*, 14−18.
(73) Lin, H.; Long, J.; Gu, Q.; Zhang, W.; Ruan, R.; Li, Z.; Wang, X. In situ IR study of Surface Hydroxyl Species of Dehydrated TiO_2:

Towards Understanding Pivotal Surface Processes of TiO_2 Photocatalytic Oxidation of Toluene. *Phys. Chem. Chem. Phys.* **2012**, *14*, 9468−9474.
(74) Lira, E.; Wendt, S.; Huo, J.; Hansen, J. Ø.; Streber, R.; Porsgaard, S.; Wei, Y.; Bechstein, R.; Lægsgaard, E.; Besenbacher, F. The Importance of Bulk Ti^{3+} Defects in the Oxygen Chemistry on Titania Surfaces. *J. Am. Chem. Soc.* **2011**, *133*, 6529−6532.